

TONE DEPENDENT COLOR ERROR DIFFUSION

Vishal Monga and Brian L. Evans

Embedded Signal Processing Laboratory, Center for Perceptual Systems
The University of Texas at Austin, Austin, TX 78712
{vishal,bevans}@ece.utexas.edu

ABSTRACT

Conventional grayscale error diffusion halftoning produces worms and other objectionable artifacts. Tone dependent error diffusion (Li and Allebach) reduces these artifacts by controlling the diffusion of quantization errors based on the input graylevel. Li and Allebach design error filter weights and thresholds for each (input) graylevel optimized based on a human visual system (HVS) model. This paper extends tone dependent error diffusion to color. In color error diffusion, what color to render becomes a major concern in addition to finding optimal dot patterns. We present a visually optimum design approach for input level (tone) dependent error filters (for each color plane). The resulting halftones reduce traditional error diffusion artifacts and achieve greater accuracy in color rendition.

1. INTRODUCTION

Digital halftoning transforms a continuous tone image (grayscale or color) to an image with a reduced number of levels for display (or printing). Examples include converting an 8-bit per pixel grayscale image to a binary image, and a 24-bit color image (with 8 bits per pixel per color) to a 3-bit color image.

In grayscale halftoning by error diffusion, each grayscale pixel is thresholded to white or black, and the quantization error is fed back, lowpass filtered, and added to neighboring grayscale pixels [1]. The feedback arrangement causes the quantization error to be high-pass filtered, i.e. pushed into high frequencies where the human eye is least sensitive. Grayscale error diffusion introduces nonlinear distortion (worms/false textures), linear distortion (sharpening) and additive noise [2].

Many variations and enhancements on grayscale error diffusion have been developed to improve halftone quality. Examples include using variable thresholds [3, 4, 5], variable filter weights [6] and different scan paths [7]. Tone dependent methods [8, 9] use error filters with different coefficients for different graylevels in

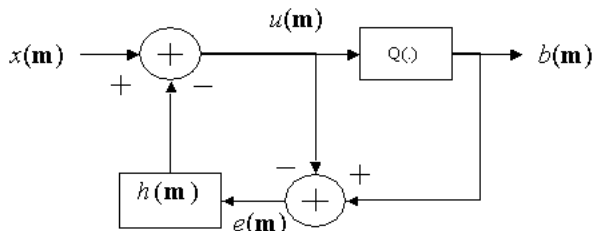


Figure 1: System block diagram for grayscale error diffusion halftoning where \mathbf{m} represents a two-dimensional spatial index (m_1, m_2)

the input image. The quantizer threshold is also modulated based on the input graylevel [8].

In this paper, we formulate the design of tone dependent color error diffusion halftoning systems. We train error filters for each color plane in order to minimize the perceived error between a constant-valued continuous-tone color image and its corresponding halftone pattern. A color HVS model takes into account the correlation among color planes. The HVS model is based on a transformation to Linearized CIELab color space [10] and exploits the spatial frequency sensitivity variation of the luminance and chrominance channels. The efficacy of Linearized CIELab in computing color reproduction errors in halftoning is shown in [11]. The resulting halftones have reduced artifacts (worms and false textures), improved accuracy in color rendition, and reduced visibility of the halftone pattern.

Color images in this paper are available at

www.ece.utexas.edu/~bevans/papers/2004/colorTDED

2. GRAYSCALE TONE DEPENDENT ERROR DIFFUSION

The system block diagram for grayscale error diffusion is shown in Fig. 1. Grayscale tone dependent error diffusion (TDED) methods use error filters $h(\mathbf{m})$ with different sizes and coefficients for different graylevels [8, 9]. The TDED algorithm [8] searches for error filter

weights and thresholds to minimize a visual cost function for each input graylevel. For the error filter design, the objective spectrum is the spectrum of the graylevel patch for highlights and shadows (graylevels 0–20 and 235–255). For input graylevel values in the midtones (graylevels 21–234), the spectrum of the direct binary search (DBS) pattern is used instead. DBS [12] produces high quality halftones by searching for the best binary pattern to match a given grayscale image by minimizing a visual distortion criterion. The authors argue that using such a design procedure error filters can be trained to produce halftone quality approaching that of DBS. The resulting halftones in [8] are shown to overcome most artifacts associated with traditional grayscale error diffusion.

For color error diffusion, independent design for each color plane would ignore the correlation among color planes. Ideally, the quantization must also be performed in a perceptual space so that every pixel can be halftoned to the nearest “perceived” color. The goal is to diffuse the color quantization error to colors and frequencies to which the HVS is least sensitive.

3. PERCEPTUAL MODEL

This section describes the model for calculating the perceived halftone in Linearized CIELab color space using the frequency responses of a channel-separable HVS.

3.1. Linearized Uniform Color Space

Linearized CIELab color space is obtained by linearizing the CIELab space about the D65 white point [10]:

$$Y_y = 116 \frac{Y}{Y_n} - 16 \quad (1)$$

$$C_x = 500 \left[\frac{X}{X_n} - \frac{Y}{Y_n} \right] \quad (2)$$

$$C_z = 200 \left[\frac{Y}{Y_n} - \frac{Z}{Z_n} \right] \quad (3)$$

The Y_y component is proportional to luminance and C_x and C_z components are similar to the red–green and blue–yellow opponent color chrominance components on which Mullen’s data [13] is based. The original CIEXYZ to CIELab transformation is non-linear [14]. This nonlinear transformation distorts the spatially averaged tone of the images, which yields halftones with incorrect average values [10]. The linearized color space overcomes this, and has the added benefit that it decouples the effect of incremental changes in (Y_y, C_x, C_z) at the white point on (L, a, b) values:

$$\nabla_{(Y_y, C_x, C_z)}(L^*, a^*, b^*)|_{D65} = \frac{1}{3} \mathbf{I} \quad (4)$$

3.2. Human Visual Frequency Response

Nasanen and Sullivan [15] chose an exponential function to model the luminance frequency response

$$W_{(Y_y)}(\tilde{\rho}) = K(L)e^{-\alpha(L)\tilde{\rho}} \quad (5)$$

where L is the average luminance of display, $\tilde{\rho}$ is the radial spatial frequency, $K(L) = aL^b$ and $\alpha(L) = \frac{1}{c \ln(L) + d}$. The frequency variable $\tilde{\rho}$ is defined [10] as a weighted magnitude of the frequency vector $\mathbf{u} = (u, v)^T$, where the weighting depends on the angular spatial frequency ϕ [15]. Thus,

$$\tilde{\rho} = \frac{\rho}{s(\phi)} \quad (6)$$

where $\rho = \sqrt{u^2 + v^2}$ and

$$s(\phi) = \frac{1 - \omega}{2} \cos(4\phi) + \frac{1 + \omega}{2} \quad (7)$$

The symmetry parameter ω is 0.7, and $\phi = \arctan(\frac{v}{u})$. The weighting function $s(\phi)$ effectively reduces the contrast sensitivity to spatial frequency components at odd multiples of 45° . The contrast sensitivity of the human viewer to spatial variations in chrominance falls off faster as a function of increasing spatial frequency than does the response to spatial variations in luminance [16]. Our chrominance model reflects this [17]:

$$W_{(C_x, C_z)}(\rho) = Ae^{-\alpha\rho} \quad (8)$$

Both the luminance and chrominance response are low-pass in nature but only the luminance response is reduced at odd multiples of 45° . This will place more luminance error across the diagonals in the frequency domain where the eye is less sensitive. Using this chrominance response as opposed to identical responses for both luminance and chrominance will allow more low frequency chromatic error, which will not be perceived by the human viewer.

4. COLOR TONE DEPENDENT ERROR DIFFUSION

4.1. Perceptual Error Metric

We train error filters to minimize a visually weighted squared error between the magnitude spectra of a “constant” input color image and its halftone pattern. Let $x_{(R,G,B)}(\mathbf{m})$ and $b_{(R,G,B)}(\mathbf{m})$ denote the constant valued continuous tone and halftone images, respectively. The calculation of the perceptual error metric is illustrated in Fig. 2. $x_{(Y_y, C_x, C_z)}(\mathbf{m})$ and $b_{(Y_y, C_x, C_z)}(\mathbf{m})$ are obtained by transforming $x_{(R,G,B)}(\mathbf{m})$ and $b_{(R,G,B)}(\mathbf{m})$ to the $Y_y C_x C_z$ space. The difference in their spectra

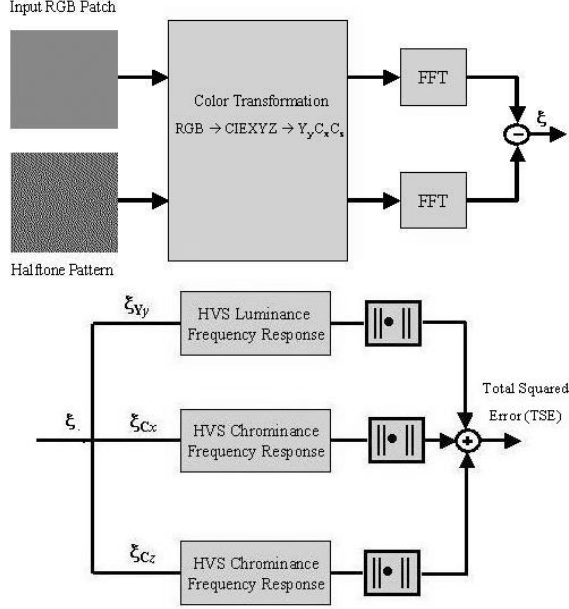


Figure 2: Block diagram for calculating the perceptual error metric.

$\xi(k, l)$ is then computed as $\xi(k, l) = \mathbf{X}_{(Y_y, C_x, C_z)}(k, l) - \mathbf{B}_{(Y_y, C_x, C_z)}(k, l)$ where

$$\mathbf{X}_{(Y_y, C_x, C_z)}(k, l) = FFT(x_{(Y_y, C_x, C_z)}(\mathbf{m})) \quad (9)$$

$$\mathbf{B}_{(Y_y, C_x, C_z)}(k, l) = FFT(b_{(Y_y, C_x, C_z)}(\mathbf{m})) \quad (10)$$

where FFT is the fast Fourier transform.

HVS filters in Section 3.2 are applied to the luminance and chrominance components of the error image in the spatial frequency domain. This corresponds to a multiplication of the filter and error image spectra $\mathbf{P}(k, l) = \xi(k, l)\mathbf{H}_{HVS}(k, l)$. Here, $\mathbf{H}_{HVS}(k, l)$ denotes the FFT of the human visual spatial filter. Note $\mathbf{P}(k, l)$, $\mathbf{H}_{HVS}(k, l)$ and $\xi(k, l)$ are vector-valued:

$$\xi(k, l) = (\xi_{Y_y}(k, l), \xi_{C_x}(k, l), \xi_{C_z}(k, l)) \quad (11)$$

$$\mathbf{H}_{HVS}(k, l) = (H_{Y_y}(k, l), H_{C_x}(k, l), H_{C_z}(k, l)) \quad (12)$$

$$\mathbf{P}(k, l) = (P_{Y_y}(k, l), P_{C_x}(k, l), P_{C_z}(k, l)) \quad (13)$$

We define the perceived error metric as the total squared error (TSE) given by

$$\sum_k \sum_l |P_{Y_y}(k, l)|^2 + |P_{C_x}(k, l)|^2 + |P_{C_z}(k, l)|^2 \quad (14)$$

4.2. Formulation of the Design Problem

The design problem is to obtain error filters for each color plane that minimize the TSE in (14), subject to the constraint that all quantization error be diffused

$$\sum_{\mathbf{k} \in \mathcal{S}} h_m(\mathbf{k}; a) = 1, h_m(\mathbf{k}; a) \geq 0 \quad \forall \quad \mathbf{k} \in \mathcal{S} \quad (15)$$

where the subscript m takes on values R , G and B , and hence, the constraints are imposed on error filters in each of three color planes. The error filter coefficients are a function of the input level a . The design objective is to obtain error filter weights for each (R, G, B) vector in the input. For 24-bit color images, this would amount to a total of 256^3 input combinations. Designing this many error filters is somewhat impractical. Instead, we consider input values along the diagonal (or neutral color) line of the color cube; i.e., $(R, G, B) = ((0, 0, 0), (1, 1, 1), \dots, (255, 255, 255))$. This results in 256 error filters for each color plane. There are two reasons for such an approach. First, the eye is particularly sensitive to colors near neutrals. Second, to a first-order approximation, the correlation among the color planes is taken into account.

The TSE as defined in (14) is, in general, not a convex function. Hence, a global minimum cannot be guaranteed. The space of solutions (error filter weights), however, comprises a convex set. The algorithm to search for the error filter weights is described in [8]. The design is based on the four-tap Floyd-Steinberg [1] support for the error filter.

5. RESULTS

Fig. 3 shows a color ramp and three different color halftones. In Fig. 3(b), false textures in the Floyd-Steinberg halftone are prominent in the middle of the yellow region (a third of the ramp length from the left) and in the center of the ramp (where yellow turns into blue). These are nearly absent in the halftone generated by the proposed color TDED method Fig. 3(d). In addition, the color TDED halftone does not suffer from directional artifacts such as diagonal worms, which appear in the yellow and blue extremes of the Floyd-Steinberg halftone. The choice of color to render is also better for the color TDED halftone. In Fig. 3(b), white dots are rendered in the blue region. These are replaced by a mixture of magenta, cyan and black dots in the color TDED halftone which are less visible.

By virtue of the design in [8], traditional error diffusion artifacts viz. worms and false textures are almost completely removed in Fig. 3(c). The halftone textures in Fig. 3(c) are also homogeneous. However, the color rendition is similar to that of Floyd-Steinberg error diffusion in Fig. 3(b). This is expected because the separable design for each color plane does not necessarily shape the color noise to frequencies of least visual sensitivity. Detail of the halftones in Fig. 3(b), (c) and (d) are shown in Fig. 4(a), (b) and (c). Note the significant improvement in the reduction of color halftone noise in Fig. 4(c) over Figs. 4 (a) and (b).

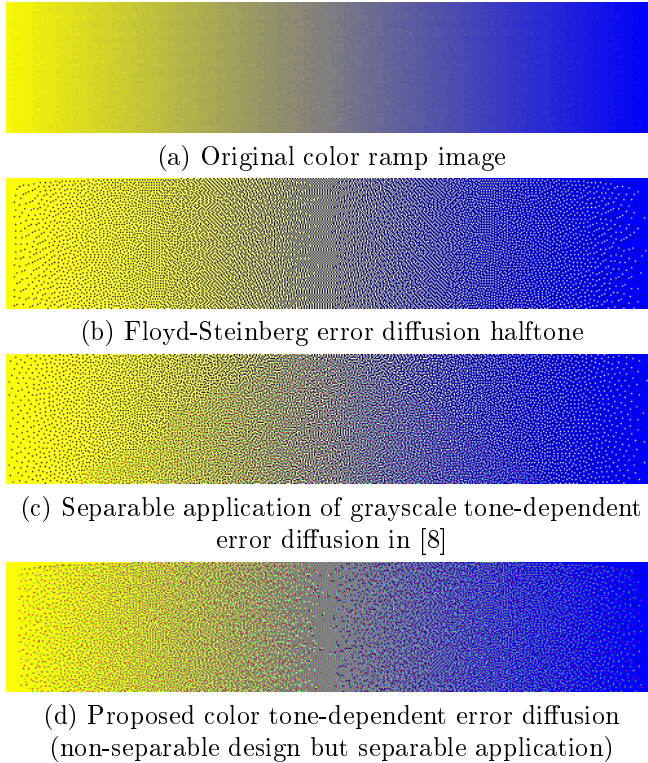


Figure 3: Color ramp and its halftone images. The halftone in (c) is courtesy of Prof. Jan Allebach and Mr. Ti-chiun Chang at Purdue University.

In addition to using different error filter coefficients, error filter shape and size may also be varied for color diffusion based on the input level, e.g. wider filters for extreme levels [8, 18]. The role of the color HVS model in minimizing visibility of color quantization noise is elaborated in [18]. To improve the homogeneity of halftone textures further, color DBS [19] may be incorporated in the design of tone dependent color error filters.

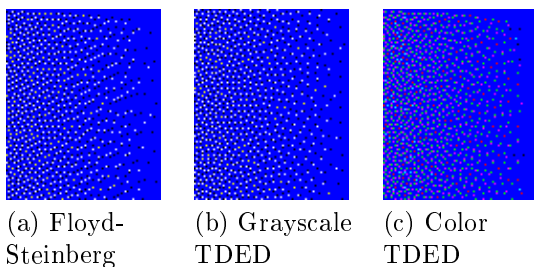


Figure 4: Detail of halftones in Fig. 3 for part of the blue portion of the color ramp.

6. REFERENCES

- [1] R. Floyd and L. Steinberg, "An adaptive algorithm for spatial grayscale," *Proc. Soc. Image Display*, vol. 17, 1976.
- [2] B. L. Evans, V. Monga, and N. Damera-Venkata, "Variations on error diffusion: Retrospectives and future trends," *Proc. SPIE Color Imaging: Processing, Hardcopy and Applications VIII*, vol. 5008, pp. 371–389, Jan. 2003.
- [3] N. Damera-Venkata and B. L. Evans, "Adaptive threshold modulation for error diffusion halftoning," *IEEE Trans. on Image Processing*, vol. 10, no. 1, pp. 104–116, Jan. 2001.
- [4] J. Sullivan, R. Miller, and G. Pios, "Image halftoning using a visual model in error diffusion," *J. Opt. Soc. Am. A*, vol. 10, no. 8, pp. 1714–1724, Aug. 1993.
- [5] R. Eschbach, "Error-diffusion algorithm with homogeneous response in highlight and shadow areas," *J. Electronic Imaging*, vol. 6, pp. 1844–1850, July 1997.
- [6] P. Wong, "Adaptive error diffusion and its application in multiresolution rendering," *IEEE Trans. on Image Processing*, vol. 5, no. 7, pp. 1184–1196, July 1996.
- [7] R. Ulichney, *Digital Halftoning*, MIT Press, 1987.
- [8] P. Li and J. P. Allebach, "Tone dependent error diffusion," *SPIE Color Imaging: Device Independent Color, Color Hardcopy, and Applications VII*, vol. 4663, pp. 310–321, Jan. 2002.
- [9] R. Eschbach, "Reduction of artifacts in error diffusion by means of input-dependent weights," *J. Electronic Imaging*, vol. 2, no. 4, pp. 352–358, Oct. 1993.
- [10] T. J. Flohr, B. W. Kolpatzik, R. Balasubramanian, D. A. Carrara, C. A. Bouman, and J. P. Allebach, "Model based color image quantization," *Proc. SPIE Human Vision, Visual Proc. and Digital Display IV*, 1993.
- [11] V. Monga, W. S. Geisler, and B. L. Evans, "Linear, color separable, human visual system models for vector error diffusion halftoning," *IEEE Signal Processing Letters*, vol. 10, pp. 93–97, Apr. 2003.
- [12] M. Analoui and J. Allebach, "Model based halftoning using direct binary search," *Proc. SPIE Human Vision, Visual Processing, and Digital Display III*, Feb. 1992.
- [13] K.T. Mullen, "The contrast sensitivity of human color vision to red-green and blue-yellow chromatic gratings," *Journal of Physiology*, 1985.
- [14] M. D. Fairchild, *Color Appearance Models*, Addison-Wesley, 1998.
- [15] J. Sullivan, L. Ray, and R. Miller, "Design of minimum visual modulation halftone patterns," *IEEE Trans. on Systems, Man, and Cybernetics*, vol. 21, no. 1, pp. 33–38, Jan. 1991.
- [16] D. H. Kelly, "Spatiotemporal variation of chromatic and achromatic contrast thresholds," *Journal Opt. Soc. Amer. A*, vol. 73, pp. 742–750, 1983.
- [17] B. Kolpatzik and C. Bouman, "Optimized error diffusion for high quality image display," *Journal of Electronic Imaging*, vol. 1, pp. 277–292, Jan. 1992.
- [18] V. Monga, N. Damera-Venkata, and B. L. Evans, "An input-level dependent approach to color error diffusion," *Proc. SPIE Color Imaging: Processing, Hardcopy and Applications IX*, Jan. 2004, accepted for publication.
- [19] U. A. Agar and J. Allebach, "Model based color halftoning using direct binary search," *Proc. SPIE Color Imaging: Processing, Hardcopy and Applications VI*, 2000.